

Assessment of the impedance cardiogram recorded by an automated external defibrillator during clinical cardiac arrest*

Nick Alexander Cromie, MD; John Desmond Allen, MD; César Navarro, PhD; Colin Turner, PhD; John McC Anderson, MPhil, DPhil; A. A. Jennifer Adgey, FACC

Objective: To assess the impedance cardiogram recorded by an automated external defibrillator during cardiac arrest to facilitate emergency care by lay persons. Lay persons are poor at emergency pulse checks (sensitivity 84%, specificity 36%); guidelines recommend they should not be performed. The impedance cardiogram (dZ/dt) is used to indicate stroke volume. Can an impedance cardiogram algorithm in a defibrillator determine rapidly circulatory arrest and facilitate prompt initiation of external cardiac massage?

Design: Clinical study.

Setting: University hospital.

Patients: Phase 1 patients attended for myocardial perfusion imaging. Phase 2 patients were recruited during cardiac arrest. This group included nonarrest controls.

Interventions: The impedance cardiogram was recorded through defibrillator/electrocardiographic pads oriented in the standard cardiac arrest position.

Measurements and Main Results: Phase 1: Stroke volumes from gated myocardial perfusion imaging scans were correlated with parameters from the impedance cardiogram system (dZ/dt_{max} and the peak amplitude of the Fast Fourier Transform of dZ/dt between 1.5 Hz and 4.5 Hz). Multivariate analysis was performed to fit stroke volumes from gated myocardial perfusion

imaging scans with linear and quadratic terms for dZ/dt_{max} and the Fast Fourier Transform to identify significant parameters for incorporation into a cardiac arrest diagnostic algorithm. The square of the peak amplitude of the Fast Fourier Transform of dZ/dt was the best predictor of reduction in stroke volumes from gated myocardial perfusion imaging scans (range = 33–85 mL; $p = .016$). Having established that the two pad impedance cardiogram system could detect differences in stroke volumes from gated myocardial perfusion imaging scans, we assessed its performance in diagnosing cardiac arrest. Phase 2: The impedance cardiogram was recorded in 132 “cardiac arrest” patients (53 training, 79 validation) and 97 controls (47 training, 50 validation): the diagnostic algorithm indicated cardiac arrest with sensitivities and specificities (\pm exact 95% confidence intervals) of 89.1% (85.4–92.1) and 99.6% (99.4–99.7; training) and 81.1% (77.6–84.3) and 97% (96.7–97.4; validation).

Conclusions: The impedance cardiogram algorithm is a significant marker of circulatory collapse. Automated defibrillators with an integrated impedance cardiogram could improve emergency care by lay persons, enabling rapid and appropriate initiation of external cardiac massage. (Crit Care Med 2010; 38:510–517)

KEY WORDS: impedance cardiogram; Fourier analysis; pulse check; cardiopulmonary resuscitation

Pulse checks by lay persons delay resuscitation and are poor indicators of cardiac arrest (sensitivity = 84%; specificity = 36%), causing an average delay of

24 secs (1–3). This low specificity indicates detection of a “pulse” when it is truly absent and will delay initiation of effective cardiopulmonary resuscitation (CPR). The current International Liaison Committee on Resuscitation/Emergency Cardiovascular Care (ILCOR/ECC) guidelines dictate that lay persons should not check for a pulse during assessment of collapsed patients (1, 2, 4, 5).

ECC training programs and public access defibrillator schemes (6–8) have been provided to lay personnel skilled in applying transthoracic electrodes and using automated external defibrillators (AEDs). How can automated defibrillator systems recognize circulatory arrest in addition to diagnosing cardiac rhythm? A hemodynamic sensor automatically diagnosing cardiac arrest, together with current electrocardiogram (ECG) algorithms, would aid in the management of

collapsed patients, where critical decisions must be made. ECG algorithms are unable to distinguish pulseless electrical activity (PEA) from sinus rhythm. In ventricular tachycardia, hemodynamic disturbance dictates immediate defibrillation. ILCOR has identified the recognition of cardiac arrest and its causes as an important scientific target for improved management of resuscitation (9).

Recent improvements in recording methods have led to widespread use of impedance cardiogram (ICG) in critical care (10–12). However, four-electrode systems are impracticable in out-of-hospital patients with cardiac arrest (13).

Our objective in this clinical study was to develop and assess a simplified defibrillator-based ICG algorithm as a hemodynamic marker of cardiac arrest, using ICG recordings from two transthoracic ECG/defibrillation pads.

*See also p. 712.

From the Department of Cardiology (NAC, CN, AAJA), Belfast Heart Centre, Royal Victoria Hospital, Belfast, Northern Ireland; Department of Physiology (JDA), Queen’s University, Belfast, Northern Ireland; Northern Ireland Bio-Engineering Centre (JMA), University of Ulster, Ulster, Northern Ireland; and the School of Electrical and Mechanical Engineering (CT), University of Ulster, Ulster, Northern Ireland.

Professor Anderson is Senior Vice-President (Science and Engineering), Heartsine Technologies. Dr. Cromie was sponsored by Research and Development Office, DHSSPS Northern Ireland, UK. The remaining authors have not disclosed any potential conflicts of interest.

For information regarding this article, E-mail: nacromie@doctors.org.uk

Copyright © 2010 by the Society of Critical Care Medicine and Lippincott Williams & Wilkins

DOI: 10.1097/CCM.0b013e3181c02ca1

MATERIALS AND METHODS

Changes in the transthoracic impedance are related mainly to variations in arterial and not cardiac blood volume (14). The theoretical basis for the standard method of ICG recording has been developed by Woltjer et al and Kubicek et al (15, 16). The standard ICG requires four electrodes, with separate electrode pairs for current application and recording to determine changing transthoracic impedance (17, 18). Recording the ICG through two defibrillation pads may have limitations. Only a vector of total transthoracic impedance is recorded, as the computed ICG signal is less specific and new analysis methods are required.

An experimental defibrillator was constructed (Samaritan AED; HeartSine Technologies, UK) to determine the ICG from a low-amplitude sinusoidal current (30 kHz; 0.05 mA) between the two defibrillator pads (19), and defibrillate (CE mark standard). Adhesive defibrillator pads (Samaritan, SDE 201, HeartSine Technologies, UK), in standard cardiac arrest positions (inferior to right clavicle in midclavicular line, to right of upper sternum, and over left lower chest), monitored ECG and ICG. The ECG, ICG, and defibrillator shocks were digitized and stored for later analysis, as established in the laboratory setting (19).

Clinical Studies

Phase 1: Comparison of the ICG with Radioisotope Determined Stroke Volume

A total of 73 patients, receiving diagnostic radioisotope myocardial perfusion imaging, were recruited between November 2003 and May 2004. The study complied with the Declaration of Helsinki. Ethical approval was obtained from the Local Regional Ethical Committee. Informed consent was obtained from the patients, who could withdraw consent at any time.

ECG and the Z/t impedance signal were recorded on a laboratory computer (digitization 1kHz; BioBench, National Instruments, Berkshire, UK). The first-order derivative (dZ/dt) was obtained retrospectively (BioBench). Channels were calibrated daily. Breath was held at peak expiration during recordings.

Stroke volumes (SV_{gated}) were determined, using gated images obtained from the gamma camera (Vision-DST XL; SMV, Buc, France) for comparison with the simultaneous ICG recordings.

Stroke volume is proportional to dZ/dt_{max} , the maximum negative deflection of the first-order derivative (Ωs^{-1}) (17). Records were analyzed in 5-sec windows and dZ/dt_{max} was determined at a filter bandwidth of 1 Hz to 11

Hz. The ICG was then studied by Fast Fourier Transformation (FFT) of the dZ/dt waveform and the peak amplitude (dB.ohms.rms) between 1.5 Hz and 4.5 Hz recorded (BioBench, National Instruments).

Multivariate analysis was performed to fit SV_{gated} with linear and quadratic terms for both dZ/dt_{max} and the peak amplitude of the FFT of dZ/dt between 1.5 Hz and 4.5 Hz. The most significant impedance parameter was incorporated into the diagnostic cardiac arrest algorithm for Phase 2 of this study (R version 2.7.1, $p < .05$ considered significant).

Phase 2: Cardiac Arrest

The ICG was recorded in 132 cardiac arrest patients attended within the hospital and in the community, by our emergency medical team (EMT) from May 1, 2003 to December 31, 2004. The adhesive ECG/ICG/defibrillator pads were placed in the standard clinical positions and the modified Samaritan AED was attached. The study complied with the Declaration of Helsinki. Ethical approval was obtained from the Local Regional Ethical Committee. All survivors (and the next-of-kin of nonsurvivors) were informed retrospectively by a letter, and could withdraw consent for the use of their data. No interruption was made in patient management during this study.

In addition, 97 controls (73 patients from Phase 1 and an additional 24 healthy individuals) provided the nonarrest records for a sustained circulation. This group included patients with a low cardiac output and cardiac symptoms referred for myocardial perfusion imaging.

The output status from the ECG, using EMT documentation, was identified by an investigator blinded to the ICG. Sinus rhythm (SR), atrial fibrillation (AF), ventricular tachycardia (VT) (pulseless and nonpulseless), ventricular fibrillation (VF), PEA, agonal rhythms, and asystole were noted. Ambiguous rhythms with artifact or incomplete documentation (i.e., PEA or SR) and no identified cardiac output status were labeled "miscellaneous." ECG and ICG records distorted by artifacts caused by CPR were excluded from the analysis.

Data were divided into training and validation sets. The training set consisted of 53 cardiac arrest patients and 47 nonarrest patients. The balance between sensitivity and specificity was used to determine the best cutoff for the algorithm on the data from the training set. A sensitivity greater than the untrained first responder, i.e., $\geq 84\%$, was considered acceptable (3). The validation set had 79 arrest patients and 50 nonarrest patients. The validation set was then tested with the algorithm developed from the training set data.

FFT analysis is not easily applied on-line in a real-time emergency defibrillator. Therefore, an alternative approach of selective filtering was adopted for frequency analysis in Phase 2. Each dZ/dt trace, both for cardiac arrest and control patients, was analyzed in 4-sec epochs. The dZ/dt signal was passed through multiple band-pass software filters (range = 1–5 Hz at frequency steps of 0.166 Hz). For each frequency, the root mean square (RMS) amplitude of the filtered signal was obtained. The dimensionless ratio of the RMS for each frequency band of the filtered signal to the RMS of the complete, unfiltered dZ/dt signal was determined. The maximum ratio from any of these frequency bands (always < 1.0) was converted into decibel units (20Log_{10}), termed PM, and squared as PM^2 , to give the equivalent of the best parameter in Phase 1. A low PM^2 was consistent with sustained cardiac output (CO).

Sustained CO has a large amplitude signal at a dominant frequency consistent with that of the heart rate. This coherent signal gives a maximum ratio (near 1.0) at close to the heart rate frequency. With conversion to decibel units, a value close to 1.0 becomes near to zero, so PM^2 will be small. In contrast, the loss of CO gives a low-amplitude signal lacking a dominant frequency. When filtered using bandwidth filters, the ratio for signal amplitude is small across the frequency range, with a large negative reduction in the decibel scale, so PM^2 will be large in the absence of CO. Because this ratiometric method is calibrated to total ICG signal amplitude, it will be less affected by variations in signal amplitude due to body habitus and electrode orientation.

The ICG algorithm (Fig. 1) used both PM^2 and the RMS of the unfiltered dZ/dt signal (Ωs^{-1}) for each epoch to assess the presence or absence of CO. Each epoch was analyzed first independently and second in conjunction with its two preceding epochs as three consecutive 4-sec epochs. The diagnosis of circulatory arrest was finally confirmed or refuted by the algorithm when similar results were obtained in two of the three consecutive epochs. If only two consecutive epochs were available, they were excluded from the triplicate analysis. The output from the diagnostic algorithm during each consecutive triplet of 4-sec epochs (12 secs) was compared with the original clinical diagnosis of the presence or absence of CO, as determined from the ECG and medical documentation. The sensitivity and specificity of the diagnostic algorithm were then calculated for both training and validation sets (SPSS 12.0.1 for Windows; SPSS, Chicago, IL). Because of small numbers in some groups, exact confidence intervals were calculated, using R version 2.7.1.

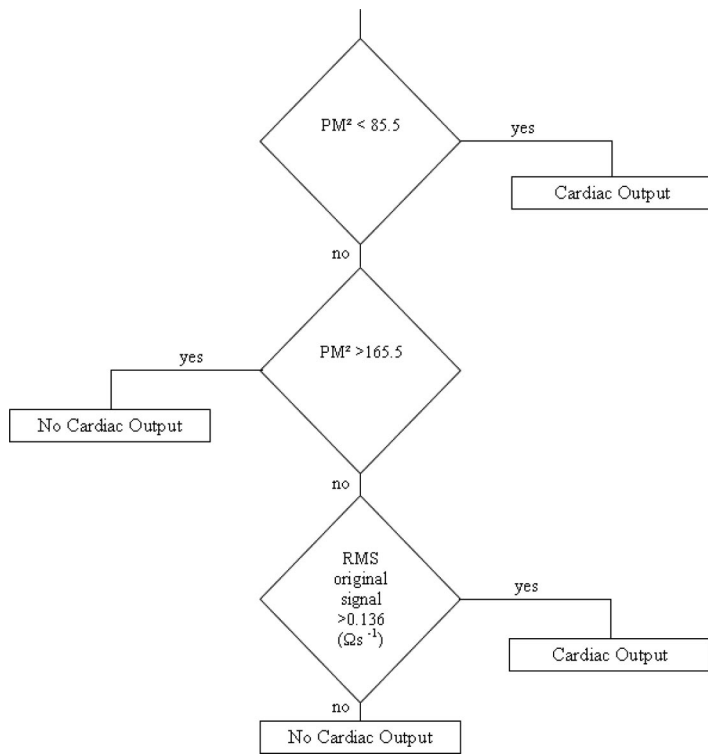


Figure 1. The automatic external defibrillator algorithm for the impedance cardiogram recorded through 2 electrocardiogram/defibrillation pads used to assess the presence or absence of cardiac output for each 4-sec epoch in phase 2. PM^2 , the square of the maximum ratio of the root mean square (RMS) of the filtered signal to that of the unfiltered signal after conversion to decibel units.

RESULTS

The ICG system can respond to altered circulatory status, as shown by sample ECG and ICG tracings in Figures 2 and 3.

Figure 2 shows both the ECG and ICG for a 61-yr-old male patient successfully resuscitated from VF. During VF, the ECG and ICG recordings show low-amplitude ICG oscillations (Fig. 2a). After restoration of SR, the ICG trace confirms the return of CO (Fig. 2b). Although both the ECG and ICG signals show oscillations during each rhythm, the ICG amplitude is larger with a more regular frequency during SR. This was indicated by a decrease in $(PM)^2$ from 597 in VF to 2.14 in SR.

The ECG and ICG for shockable (pulseless) VT and nonshockable (palpable pulse) VT can be compared in two different patients (Fig. 3). Figure 3a shows shockable VT, confirmed by our EMT, requiring immediate direct current (DC) cardioversion in a male patient with myocardial ischemia. Circulatory arrest was confirmed by $(PM)^2$ of 230. In Fig. 3b, from a patient without myocardial infarction (male, age = 58 yrs), VT was present

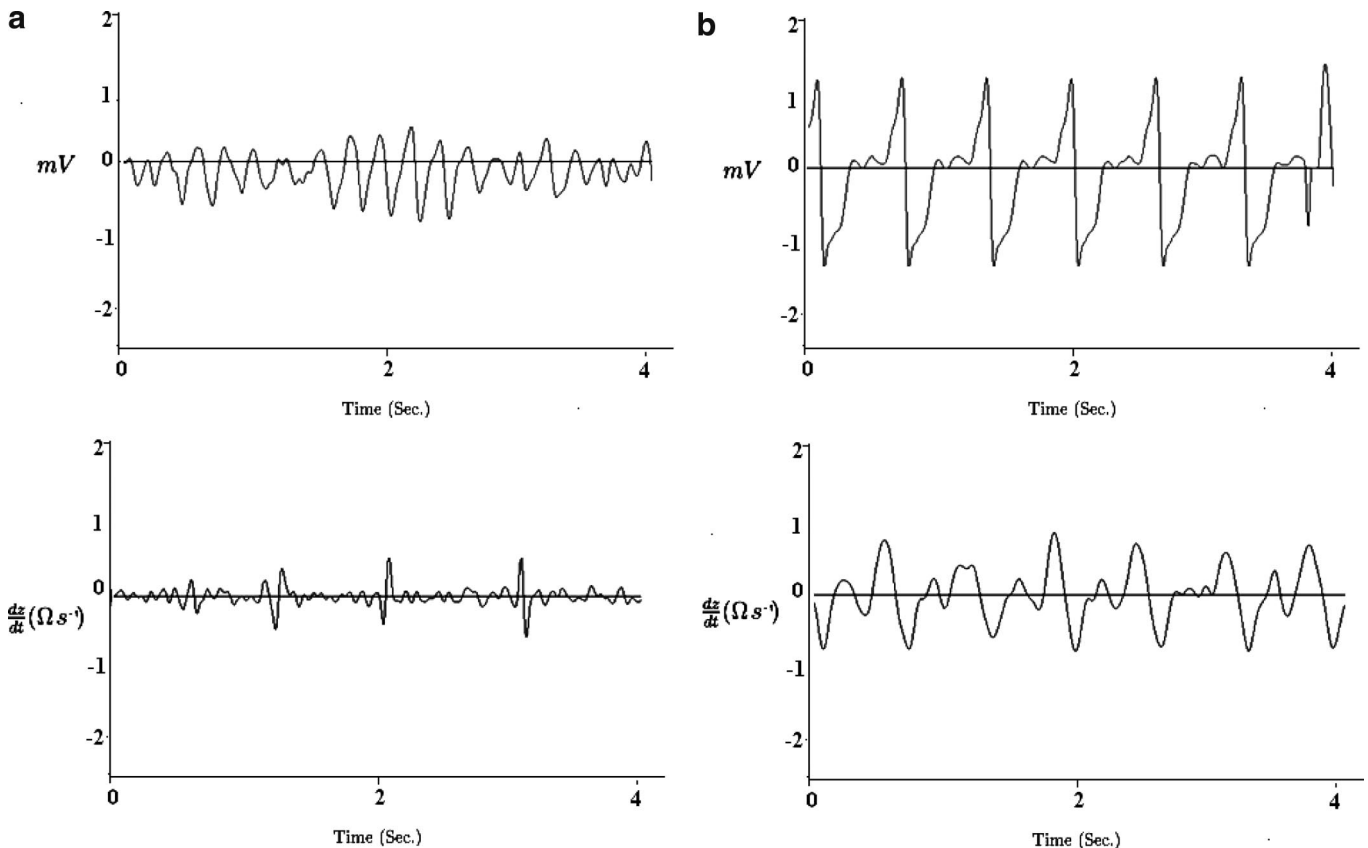


Figure 2. Two 4-sec records show the electrocardiogram (top) and the impedance cardiogram (bottom; as dZ/dt), from 2 electrocardiogram/defibrillation pads in a 61-yr-old male patient during ventricular fibrillation (a) and after successful defibrillation into sinus rhythm (b).

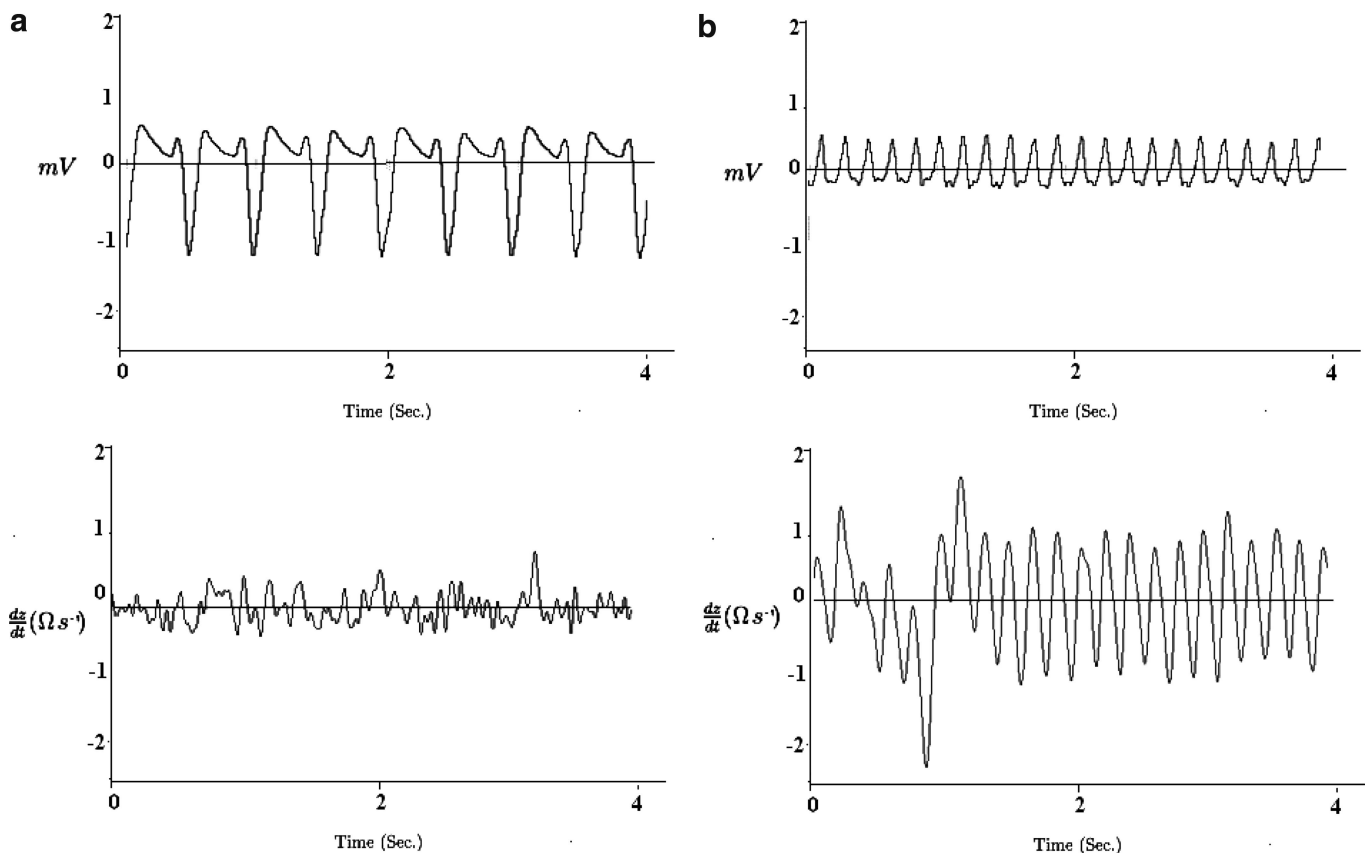


Figure 3. A 4-sec record showing the electrocardiogram (*top*) and the impedance cardiogram (*bottom*; as dZ/dt), recorded through 2 electrocardiogram/defibrillator pads, for a 69-yr-old male patient with myocardial ischaemia (*a*). The patient had pulseless (or shockable) ventricular tachycardia, requiring immediate cardioversion. *b*, A 58-yr-old male patient had a broad complex tachycardia and no myocardial infarction. The heart rate was 325 beats/min and systolic blood pressure 75 mm Hg, so the patient did not require immediate cardioversion.

but circulation was sustained, and he did not require immediate DC cardioversion (Fig. 3*b*). As demonstrated, both ICG signals are oscillatory during the VT but with sustained circulation, not requiring immediate DC cardioversion; the ICG amplitude is larger with a more regular frequency. In this nonshockable VT, $(PM)^2$ was 145.6 but the presence of CO was confirmed by RMS of the unfiltered dZ/dt (22.24).

Phase 1: Comparison of the ICG with Radioisotope Determined Stroke Volume

Patient and ICG parameters are summarized in Table 1, with ranges, mean and standard deviation values. Successful gated images were obtained in 71 of 73 patients (47 male, 24 female; mean age = 61.8 ± 11 yrs) (Table 1). SR was present in 60 patients. In two patients, gated images could not be obtained due to fast AF.

As correlation coefficients were weak ($r^2 = .08$, $p = .02$ for SV_{gated} and the

square of the peak amplitude of the FFT of dZ/dt between 1.5 Hz and 4.5 Hz), multivariate analysis was performed to fit SV_{gated} with both dZ/dt_{max} and the peak amplitude of the FFT of dZ/dt (between 1.5 Hz and 4.5 Hz), and all possible quadratic terms (i.e., multiples within and between parameters) (Table 2). All nonsignificant parameters were eliminated sequentially, leaving the square of the peak amplitude of the FFT of dZ/dt (between 1.5 Hz and 4.5 Hz) (Table 2 and 3). This was significant at indicating a reduction in SV_{gated} (range = 33–85 mL; $p = .016$) compared with the other impedance-derived parameters (Table 3).

Phase 2: Cardiac Arrest

The presenting rhythms for cardiac arrest and control (with sustained circulation) groups are summarized for both the training and validation sets in Table 3.

The training set had 53 cardiac arrest patients and 47 controls. In four of the “arrests,” the patients had sustained CO

on arrival (one AF and three SR) (Table 3). For the control patients, four were in AF (two with complete and one with partial left bundle-branch block) (Table 3). There were 765 cardiac arrest and 4979 noncardiac arrest 4-sec epochs, from a total of 16,900 4-sec epochs, after removal of epochs containing artifact due to CPR.

There were 79 cardiac arrest patients and 50 controls in the validation set. Two patients were labeled “miscellaneous,” having an indeterminate rhythm. In seven “arrests,” the patients had a sustained CO on arrival (three AF, three SR, and one complete heart block) (Table 3). For the control patients, one showed AF with left bundle-branch block (Table 3). There were 922 cardiac arrest 4-sec epochs and 9466 noncardiac arrest epochs remaining, from a total of 24,534 epochs after removal of CPR artifact.

Triplicate epochs were then analyzed for the cardiac arrest and nonarrest records in the training set. Confirmation of the output status required two of three epochs to be the same to confirm diag-

Table 1. Patient parameters, radioisotope determined stroke volumes and impedance cardiogram measurements (Phase 1 study)

	Range	Mean	SD
Age, yr	36–84	61.79	10.96
Height, cm	152.4–190.5	169.70	9.28
Weight, kg	51–130	81.14	15.09
SV _{gated} per beat, mL	33–85	60.75	10.84
dZ/dt _{max} , Ωs ⁻¹	0.53–2.97	1.43	0.55
Peak FFT dZ/dt between 1.5 Hz and 4.5 Hz, dB.Ohms.rms	-11.91–3.45	-4.15	3.72

Range, mean, and standard deviation (SD) values are shown for patient parameters, radioisotope-determined stroke volume (SV_{gated}), the amplitude of dZ/dt_{max} (Ωs⁻¹), and the peak amplitude of the Fast Fourier Transformation (FFT) of dZ/dt between 1.5 Hz and 4.5 Hz (dB.Ohms.rms).

The impedance cardiogram signal was recorded between two electrocardiogram/defibrillator pads in 71 patients attending for diagnostic myocardial perfusion scans.

Table 2. Multivariate comparison of impedance measurements and radioisotope determined stroke volumes (Phase 1 study)

	Estimate	SE	Significance <i>p</i>
dZ/dt _{max}	1.65984	16.0027	.918
(dZ/dt _{max}) ²	-0.47124	4.21990	.911
Peak FFT dZ/dt	-0.88449	2.31998	.704
(Peak FFT dZ/dt) ²	-0.15959	0.11721	.178
dZ/dt _{max} × Peak FFT dZ/dt	0.04557	0.94282	.962
(Peak FFT dZ/dt) ²	-0.08465	0.03430	.016

SE, standard error; FFT, Fast Fourier Transformation.

Multivariate analysis was performed to fit SV_{gated} with linear and quadratic terms for dZ/dt_{max} and the peak amplitude of the FFT of dZ/dt between 1.5 Hz and 4.5 Hz (Peak FFT dZ/dt).

Levels of significance are shown when all parameters were considered during multivariate analysis, and after sequential exclusion of the least significant parameters.

nosis (Table 4). There were 359 cardiac arrest triplicate 4-sec epochs and 4809 noncardiac arrest epochs suitable for

Table 3. Initial rhythms in training and validation sets (Phase 2)

Cardiac Arrest Rhythms	Training Set	Validation Set
Ventricular fibrillation	8	18
Ventricular tachycardia	1	6
Agonal	3	3
Pulseless electrical activity	15	20
Asystole	18	23
Miscellaneous	4	2
Sustained circulation present	4	7
Total	53	79
Control Group Rhythms		
Sinus rhythm	43	49
Atrial fibrillation	4	1
Total	47	50

Initial rhythms as determined by the Emergency Medical Team after arrival at a “cardiac arrest” and the cardiac rhythms in the control groups.

“Miscellaneous” was applied to ambiguous or indeterminate rhythms (e.g., pulseless electrical activity or sinus rhythm).

analysis. Of the 359 cardiac arrest epochs, the ICG algorithm diagnosed 320 correctly (sensitivity = 89.1%). Of the 4809 noncardiac arrest epochs, the ICG algorithm diagnosed 4789 correctly (specificity = 99.6%). The performance of the algorithm for each rhythm for triplicate epochs (Table 4) was much better than with the data for single epochs (not shown).

Similarly using triplicate epochs for analysis of cardiac arrest and nonarrest records in the validation set (Table 5), there were 561 cardiac arrest triplicate 4-sec epochs and 9095 noncardiac arrest epochs suitable for analysis. Of the 561 cardiac arrest epochs, the algorithm diagnosed 455 correctly (sensitivity = 81.1%). Of the 9095 noncardiac arrest epochs, the algorithm diagnosed 8828 correctly (specificity = 97.1%). The performance of the algorithm for each rhythm is shown in Table 5 for triplicate epochs in the validation set.

Because the QRS complex rate could affect the signal analysis of the ICG, we have shown sensitivities and specificities (± exact 95% confidence intervals [CIs])

for sinus, atrial fibrillation, and PEA at heart rates <60 beats/min (bradycardia), 61 beats/min to 100 beats/min, and >100 beats/min (tachycardia) (Table 6).

DISCUSSION

Correct and uncomplicated advice for first responders during management of the collapsed patient is crucial. How can syncopal patients with CO be differentiated from patients in cardiac arrest, e.g., due to a PEA rhythm? Can automated defibrillator algorithms distinguish a patient with pulseless VT from nonpulseless VT (Fig. 3)? Pulse checks by lay responders are unreliable and can delay effective CPR. An automated hemodynamic sensor would aid the management of such patients without requiring additional training for lay persons. However, it must show both high specificity, facilitating prompt management, and high sensitivity, not delaying correct treatment by inaccurate measurement. The traditional ICG parameters—left ventricular ejection time and baseline impedance (15, 16)—are not available in cardiac arrest. During cardiac arrest, the role of the ICG is to indicate presence or absence of CO. This has been achieved in the present studies by signal analysis methods. Multivariate analysis showed the square of the peak amplitude of the FFT of dZ/dt was best at determining a reduction in stroke volume (*p* = .016) in Phase 1 of the present study. A previous study of changes in transthoracic impedance, recorded through two defibrillation pads, showed significant but poor correlations with arterial blood pressure recordings in intubated and ventilated patients (12).

The present Phase 2 results indicate that over an assessment period of 12 secs, selective filtering of the ICG is a powerful hemodynamic sensor of cardiac arrest. The present system of two defibrillation/ECG electrodes, recording a vector rather than the standard transthoracic impedance, will cause systematic errors in the use of the Kubicek equation for stroke volume, so a new parameter was used to study the frequency component of the ICG. The high sensitivities (89%; 95% CI, 85.4–92.1% training set; 81%; 95% CI, 77.6–84.3% validation set) and high specificities (99.6%; 95% CI, 99.36–99.75% training set; 97%; 95% CI, 96.7–97.4% validation set) exceed those for detection of an absent pulse by lay persons (84% sensitivity; 36% specificity), where a decision was delayed for 24 secs

Table 4. Determination of sensitivities and specificities for analysis of triplicate epochs in training set (Phase 2)

Triplicate Epochs - Training Set					
359 Arrest Epochs: 320 Correct/39 Incorrect, Sensitivity 89.14% (95% CI, 85.4–92.1)					
4809 Nonarrest Epochs: 4789 Correct/20 Incorrect, Specificity 99.58% (95% CI, 99.36–99.75)					
Arrest Rhythms	Total	Algorithm Correct	Algorithm Incorrect	Sensitivity	Exact Lower and Upper 95% CI
Ventricular fibrillation	48	42	6	87.5	(74.8–95.3)
VT (shockable)	3	3	0	100	(–)
Agonal	20	20	0	100	(–)
PEA	175	155	20	88.6	(82.9–92.9)
Asystole	113	100	13	88.5	(81.1–93.7)
Torsade de pointes	0	0	0		
P wave asystole	0	0	0		
Total arrest rhythms	359	320	39	89.14	(85.4–92.1)
Nonarrest rhythms	Total	Algorithm Correct	Algorithm Incorrect	Sensitivity	Exact Lower and Upper 95% CI
Sinus	4288	4270	18	99.6	(99.3–99.7)
Atrial fibrillation	409	407	2	99.5	(98.2–99.9)
Sinus with broad QRS	112	112	0	100	(–)
VT (nonshockable)	0	0	0		
Complete heart block	0	0	0		
Total nonarrest rhythms	4809	4789	20	99.58	(99.4–99.7)

CI, confidence interval; VT, ventricular tachycardia; PEA, pulseless electrical activity.

Analysis of circulatory arrest and nonarrest epochs in triplicate, with two of three consecutive 4-sec epochs required to confirm diagnosis in the training set. The numbers of correct and incorrect decisions by the diagnostic algorithm confirming cardiac arrest or sustained circulation, and the calculated sensitivities and specificities with exact 95% confidence intervals are shown for different cardiac arrhythmias.

Table 5. Determination of sensitivities and specificities for analysis of triplicate epochs in validation set (Phase 2)

Triplicate Epochs - Validation Set					
561 Arrest Epochs: 455 Correct/106 Incorrect, Sensitivity 81.1 (95% CI, 77.6–84.3)					
9095 Nonarrest Epochs: 8828 Correct/267 Incorrect, Specificity 97.1 (95% CI, 96.7–97.4)					
Arrest Rhythms	Total	Algorithm Correct	Algorithm Incorrect	Sensitivity	Exact Lower and Upper 95% CI
Ventricular Fibrillation	147	123	24	83.7	(76.7–89.2)
VT (shockable)	7	3	4	42.9	(9.9–81.6)
Agonal	27	18	9	66.7	(46.0–83.4)
PEA	168	132	36	78.6	(71.6–84.5)
Asystole	209	179	30	85.6	(80.1–90.1)
Torsade de pointes	2	0	2	0	(–)
P wave asystole	1	0	1	0	(–)
Total arrest rhythms	561	455	106	81.11	(77.6–84.3)
Nonarrest rhythms	Total	Algorithm Correct	Algorithm Incorrect	Specificity	Exact Lower and Upper 95% CI
Sinus rhythm	7511	7289	222	97	(96.6–97.4)
Atrial fibrillation	1459	1414	45	96.9	(95.9–97.7)
Sinus with broad QRS	104	104	0	100	(–)
VT (nonshockable)	20	20	0	100	(–)
Complete heart block	1	1	0	100	(–)
Total nonarrest rhythms	9095	8828	267	97.06	(96.7–97.4)

CI, confidence interval; VT, ventricular tachycardia; PEA, pulseless electrical activity.

Analysis of circulatory arrest and nonarrest epochs in triplicate, with two of three consecutive 4-sec epochs required to confirm diagnosis in the validation set. The numbers of correct and incorrect decisions by the diagnostic algorithm confirming cardiac arrest or sustained circulation, and the calculated sensitivities and specificities with exact 95% confidence intervals are shown for different cardiac arrhythmias.

Table 6. Sensitivities and specificities (\pm exact 95% CI) for recognition of circulatory status at various heart rates in the training and validation sets

Rhythm	Total			Heart Rate <60 beats/min			Heart Rate 61–100 beats/min			Heart Rate >100 beats/min		
	Number	Sensitivity	Specificity	Number	Sensitivity	Specificity	Number	Sensitivity	Specificity	Number	Sensitivity	Specificity
Training												
Set												
SR	4400		99.6 (99.4–99.8)	452		99.3 (98.1–99.9)	3912		99.6 (99.3–99.8)	36		100 (–)
AF	409		99.5 (98.2–99.9)	21		100 (–)	351		99.4 (98.0–99.9)	37		100 (–)
PEA	175	88.6 (82.9–92.9)		75	84 (73.7–91.4)		54	96.3 (87.3–99.5)		46	87.0 (73.7–95.1)	
Validation												
Set												
SR	7615		97.1 (96.7–97.5)	990		99.4 (98.7–99.8)	5054		97.3 (96.8–97.7)	1571		95.0 (93.8–96.0)
AF	1459		96.9 (95.9–97.7)	57		78.9 (66.1–88.6)	595		98.8 (97.6–99.5)	807		96.8 (95.3–97.9)
PEA	168	78.6 (71.6–84.5)		83	90.4 (81.9–95.7)		56	78.6 (65.6–88.4)		29	44.8 (26.4–64.3)	

CI, confidence interval; SR, sinus rhythm; AF, atrial fibrillation; PEA, pulseless electrical activity.

Number of epochs analyzed for various rhythms at various heart rates (<60 beats/min, 61–100 beats/min, >100 beats/min), along with sensitivities and specificities (\pm exact 95% CI in parentheses), for recognition of circulatory status during SR, AF, and PEA.

on average (3). Caution should be noted here that, due to the nature of this pilot study, multiple epochs were obtained from each patient.

In our clinical study, dZ/dt_{max} was not as effective in determining cardiac arrest states as selective filtering of dZ/dt . Frequency analysis can also be used to separate the presence of CO from that of respiratory artifact caused by ventilation and agonal breathing. Both states cause fluctuations in the ICG but, as they occur at different frequencies, these can be differentiated by filtering and/or software development (20).

Our protocol has limitations. It required the accurate assessment and documentation of pulse by the EMT or cardiac arrest team on arrival and throughout the cardiac arrest. Often this is difficult, causing more “miscellaneous” rhythms to be diagnosed than anticipated in the present study. Obtaining sensitivities and specificities relies on independence between observations; however, in this study, multiple observations are obtained from each subject. In an attempt to compensate for this, exact CIs were obtained. The breakdown of algorithm performance for each triplicate epoch is summarized for both the training and validation sets (Tables 4 and 5). In the case of shockable ventricular tachycardia in the validation set, identified with 100% sensitivity in the training set, low sensitivity may be attributed to small total numbers with wide CIs. In the one patient with two triplicate epochs of torsade de pointes and no pulse identified by the EMT, the algorithm indicated a CO (Table 5). The ICG showed respiratory artifact as the patient continued to breathe during the assessment period, despite no palpable pulse.

Varying success has been achieved by other algorithms to distinguish between PEA and pulse-circulating rhythms (21, 22). An ECG algorithm alone has been reported to distinguish PEA with high sensitivity (90%) from pulse-circulating rhythms (specificity 85%) in 191 3-sec epochs from 653 cardiac arrests (21). However, this abstract does not specify how physician teams decided which ECG tracings were PEA. Even trained paramedics failed to reach 90% specificity in pulse recognition in a controlled environment (3). A small retrospective analysis (218 10-sec epochs from 653 cardiac arrest episodes) used a combined ECG/ICG algorithm and a signal averaged ICG to obtain a sensitivity of 90% and specificity of 91.5% in recognizing PEA from a pulsatile cardiac rhythm (22). Additional algorithms in development, using a similar ICG vector, found a sensitivity of 90% and specificity of 82% in detecting “insufficient circulation” in 434 epochs obtained from 69 ventilated patients: each epoch required at least nine QRS complexes for signal averaging (12). Our study, in contrast, is more comprehensive, examining all cardiac arrest incidents and rhythms with large data sets in both training and validation sets, using an ICG algorithm alone. High sensitivities were seen for pulse-circulating rhythms (sinus, AF, and broad complex) with lower specificities for PEA detection.

Many current AEDs are already equipped with an impedance channel, so this system would be easily applicable to clinical practice and could be readily implemented. As such, minimal modification would be required to the AED with no modification to the ECG/defibrillation pads as would be required by other hemodynamic sensors. The addition of an

echo transducer placed on the apical pad would not be reliable as Doppler pulse wave sensors may not be applied along the cardiac long axis. Application of pulse oximetry probes on a patient’s finger requires additional training and has the potential to confuse first responders, making resuscitation attempts less efficient.

Automated defibrillators with dynamic ICG detection, in addition to current ECG algorithms, can potentially advise bystanders to commence CPR in VF, VT, PEA, and asystolic arrests. Importantly, such devices could also monitor patients during postresuscitative care (Fig. 2). Automated signal analysis by this simple system would inform defibrillator users of circulatory status over and above that of ECG algorithms alone.

CONCLUSION

Selective filtering of the frequency spectrum of the ICG recorded through the two transthoracic defibrillator pads can be used as a marker of circulatory collapse, enabling more rapid and appropriate initiation of external cardiac massage. These studies provide the basis for further development of the ICG signal in defibrillator design and emergency clinical practice.

ACKNOWLEDGMENTS

We thank Audrey Tomlinson, RGN, and Leslie Swales, RGN, Royal Victoria Hospital, Belfast, for their help in data acquisition, and Rebecca DiMaio and Alister McIntyre, PhD, of Heartsine Technologies, Belfast, for assistance with data analysis.

REFERENCES

1. Cummins RO, Hazinski MF: The most important changes in the International ECC and CPR Guidelines 2000. *Circulation* 2000; 102:I-371–I-376
2. Cummins RO, Hazinski MF: Guidelines based on fear of type II (false-negative) errors. Why we dropped the pulse check for lay rescuers. *Circulation* 2000; 102(Suppl 1):I-377–I-379
3. Eberle B, Dick WF, Schneider T, et al: Checking the carotid pulse check: Diagnostic accuracy of first responders in patients with and without a pulse. *Resuscitation* 1996; 33: 107–116
4. 2005 American Heart Association guidelines for cardiopulmonary resuscitation and emergency cardiovascular care. Part 4: Adult basic life support. *Circulation* 2005; 112 (Suppl): IV-19–IV-34
5. Handley AJ, Becker LB, Allen M, et al: Single-rescuer adult basic life support. An advisory statement from the Basic Life Support Working Group of the International Liaison Committee on Resuscitation (ILCOR). *Circulation* 1997; 95:2174–2179
6. Capucci A, Aschieri D, Piepoli MF, et al: Tripling survival from sudden cardiac arrest via early defibrillation without traditional education in cardiopulmonary resuscitation. *Circulation* 2002; 106:1065–1070
7. Culley LL, Rea TD, Murray JA, et al: Public access defibrillation in out-of-hospital cardiac arrest. A community-based study. *Circulation* 2004; 109:1859–1863
8. van Alem AP, Vrenken RH, de Vos R, et al: Use of automated external defibrillator by first responders in out of hospital cardiac arrest: prospective controlled trial. *BMJ* 2003; 327:1312–1315
9. Scientific knowledge gaps and clinical research priorities for cardiopulmonary resuscitation and emergency cardiovascular care identified during the 2005 International Consensus Conference on ECC and CPR Science with Treatment Recommendations. A Consensus Statement from the International Liaison Committee on Resuscitation; the American Heart Association Emergency Cardiovascular Care Committee; the Stroke Council; and the Cardiovascular Nursing Council. *Resuscitation* 2007; 75:400–411
10. Packer M, Abraham WT, Mehra MR, et al: Utility of impedance cardiography for the identification of short-term risk of clinical decompensation in stable patients with chronic heart failure. *J Am Coll Cardiol* 2006; 47:2245–2252. Epub 2006 May 15
11. Mehra MR: Optimizing outcomes in the patient with acute decompensated heart failure. *Am Heart J* 2006; 151:571–579
12. Losert H, Risdal M, Sterz F, et al: Thoracic-impedance changes measured via defibrillator pads can monitor signs of circulation. *Resuscitation* 2007; 73:221–228
13. Johnston PW, Imam Z, Dempsey G, et al: The transthoracic impedance cardiogram is a potential haemodynamic sensor for an automated external defibrillator. *Eur Heart J* 1998; 19:1879–1888
14. Bonjer FH, Van Den Berg JW, Dirken MNJ: The origin of the variations of body impedance occurring during the cardiac cycle. *Circulation* 1952; 6:415–420
15. Woltjer HH, Bogaard HJ, de Vries PMJM: The technique of impedance cardiography. *Eur Heart J* 1997; 18:1396–1403
16. Kubicek WG, Kottke J, Ramos MU, et al: The Minnesota impedance cardiograph—Theory and applications. *Biomed Eng* 1974; 9:410–416
17. Bernstein DP: A new stroke volume equation for thoracic electrical bioimpedance: Theory and rationale. *Crit Care Med* 1986; 14:904–909
18. Kubicek WG: On the source of peak first time derivative (dZ/dt) during impedance cardiography. *Ann Biomed Eng* 1989; 17:459–462
19. Cromie NA, Allen JD, Turner C, et al: The impedance cardiogram recorded through two electrocardiogram/defibrillator pads as a determinant of cardiac arrest during experimental studies. *Crit Care Med* 2008; 36: 1578–1584
20. Losert H, Risdal M, Sterz F, et al: Thoracic impedance changes measured via defibrillator pads can monitor ventilation in critically ill patients and during cardiopulmonary resuscitation. *Crit Care Med* 2006; 34:2399–2405
21. Risdal M, Steen PA, Kramer-Johansen J, et al: Discriminating between PEA and pulse circulating rhythm using ECG. Abstr. *Resuscitation* 2006; 69:46
22. Risdal M, Aase SO, Kramer-Johansen J, et al: Automatic identification of return of spontaneous circulation during cardiopulmonary resuscitation. *IEEE Trans Biomed Eng* 2008; 55:60–68